# Low level laser therapy increases angiogenesis in a model of ischemic skin flap in rats mediated by VEGF, HIF-1α and MMP-2*

**Vivian Cury**[a], **Ana Iochabel Soares Moretti**[b,c,*], **Lívia Assis**[a], **Paulo Bossini**[a], **Jaqueline de Souza Crusca**[a], **Carlos Benatti Neto**[d], **Renan Fangel**[a], **Heraldo Possolo de Souza**[b], **Michael R Hamblin**[e,f,g], and **Nivaldo Antonio Parizotto**[a]

[a]Department of Physiotherapy, Federal University of São Carlos, São Carlos, São Paulo, Brazil

[b]Emergency Medicine Division, Faculdade de Medicina da Universidade de São Paulo, São Paulo, Brazil

[c]Post-Graduate Health Sciences Program, Instituto de Assistência Médica ao Servidor Público Estadual—IAMSPE, São Paulo, SP, Brazil

[d]Department of Physiology and Pathology, Universidade Estadual de São Paulo, Araraquara, São Paulo, Brazil

[e]Wellman Center for Photomedicine, Massachusetts General Hospital, Boston, MA 02114, United States

[f]Department of Dermatology, Harvard Medical School, Boston, MA 02115, United States

[g]Harvard–MIT Division of Health Sciences and Technology, Cambridge, MA 02139, United States

## Abstract

It is known that low level laser therapy is able to improve skin flap viability by increasing angiogenesis. However, the mechanism for new blood vessel formation is not completely understood. Here, we investigated the effects of 660 nm and 780 nm lasers at fluences of 30 and 40 J/cm$^2$ on three important mediators activated during angiogenesis. Sixty male Wistar rats were used and randomly divided into five groups with twelve animals each. Groups were distributed as follows: skin flap surgery non-irradiated group as a control; skin flap surgery irradiated with 660 nm laser at a fluence of 30 or 40 J/cm$^2$ and skin flap surgery irradiated with 780 nm laser at a fluence of 30 or 40 J/cm$^2$. The random skin flap was performed measuring $10 \times 4$ cm, with a plastic sheet interposed between the flap and the donor site. Laser irradiation was performed on 24 points covering the flap and surrounding skin immediately after the surgery and for 7 consecutive days thereafter. Tissues were collected, and the number of vessels, angiogenesis markers (vascular endothelial growth factor, VEGF and hypoxia inducible factor, HIF-1α) and a tissue remodeling marker (matrix metalloproteinase, MMP-2) were analyzed. LLLT increased an angiogenesis, HIF-1α and VEGF expression and decrease MMP-2 activity. These phenomena were dependent on the fluences, and wavelengths used. In this study we showed that LLLT may improve the healing of skin flaps by enhancing the amount of new vessels formed in the tissue. Both 660 nm

*Corresponding author. Address: Laboratory of Medical Research, Division of Emergency Medicine, Faculdade de Medicina, Universidade de São Paulo, Av. Dr. Arnaldo, 455 sala 3189, CEP 01246-903 São Paulo, SP, Brazil. Tel.: +55 11 30648756; fax: +55 11 30617170. aismoretti@yahoo.com.br (A.I.S. Moretti).

and 780 nm lasers were able to modulate VEGF secretion, MMP-2 activity and HIF-1α expression in a dose dependent manner.

## Keywords

LLLT; Hypoxia; Angiogenesis; HIF1-α; VEGF; MMP-2

## 1. Introduction

Skin flaps are frequently used to reconstruct large areas of skin, damaged after accidental trauma or surgical procedures, like tumor resection. Although this maneuver is generally regarded as safe, when correctly performed, complications may still occur. Considering that these grafts might represent the last resource available for treatment of injured patients, the loss of the skin flaps are devastating events.

The mostly feared of these events is skin flap necrosis, caused by inadequate blood flow [1–4]. Under ideal conditions, hypoxia resulting from improper tissue perfusion should lead to an adaptive response, inducing angiogenesis, that is, the formation of new vessels from pre-existing ones, a necessary step to ensure adequate blood supply during the healing process [5–7]. The mechanism of angiogenesis is very complex, involving several cell types and dozens of mediators and signaling pathways. This cascade of events is initiated by migration and invasion of endothelial cells, followed by lumen formation, connection of new vascular segments with pre-existing circulation, and remodeling of extracellular matrix (ECM), a process dependent on adequate matrix metalloproteinase (MMP) activity [7]. Moreover, among the many signaling pathways that are involved in the whole process, some of them seem to be particularly critical such as vascular endothelial growth factor (VEGF) and hypoxia inducible factor 1α (HIF-1α) [5].

Low level laser therapy (LLLT) has been demonstrated to be able to modulate biological mechanisms in wound healing [8,9], angiogenesis [10,11], and inflammation [12,13]. Besides that, it has also been reported to induce angiogenesis in several experimental models where blood vessel formation is critical to success [10,11]. Although LLLT has a history of widespread use and good results, the mechanism(s) for its actions are not yet completely understood. Our group has previously reported that LLLT can increase the viability of skin flaps, increasing local vascularization and reducing the area of necrosis [3]. These results have been further confirmed by other authors [2,14]. However, the mechanisms responsible for LLLT-induced revascularization have not yet been explored in detail.

Therefore, the main objective of this study was to analyze molecular mechanisms involved in LLLT-induced angiogenesis in a model of ischemic skin flap in rats. We focused our attention in some of the most important mediators involved in angiogenesis, such as VEGF and HIF-1α expression and MMP activity.

## 2. Methods

### 2.1. Skin flap surgical procedure

This study was conducted in accordance with the Guide for Care and Use of Laboratory Animals and approved by the Animal Ethics Committee of the Federal University of São Carlos [4]. Sixty adult male rats (Wistar, 12 weeks old, 260–320 g) were anesthetized by intraperitoneal injection of ketamine (95 mg/kg) and xylazine (12 mg/kg) and shaved on the dorsal region. A skin flap measuring $10 \times 4$ cm was raised with a cranial base on the back of each rat (Fig. 1A and B). A plastic barrier with the same dimensions was inserted between

the flap and its donor site (Fig. 1C). Flaps were closed with simple nylon 4/0 stitches(Fig. 1D). Laser irradiation was performed immediately after the surgery and for 4 consecutive days after surgery (Fig. 1E). A low-energy 660 nm and 780 nm laser (Twin Laser, MM Optics, São Carlos, Brazil), continuous wave (CW), 4 mm beam diameter, 40mW total power was used. Laser irradiation was performed at fluences of 30 J/cm$^2$ (30 s, total energy 28.8 J) and 40 J/cm$^2$ (40 s, total energy 38.4 J). Twenty-four points on the skin flap surface and surrounding it were irradiated through the punctual contact technique. The irradiation was performed with a plastic template that overlaid the skin flap with demarcation points covering the entire flap and 1-cm of normal skin on all sides (Fig. 1E).

All animals were submitted to a skin flap (SF) surgery procedure and randomly divided into five groups, with 12 animals each. Groups were as follows:

1.  SF-NI group, skin flap surgery non-irradiated group.

2.  SF-R30 skin flap surgery irradiated with 660 nm laser, 30 J/cm$^2$.

3.  SF-R40 skin flap surgery irradiated with 660 nm laser, 40 J/cm$^2$.

4.  SF-IV30 skin flap surgery irradiated with 780 nm laser, 30 J/cm$^2$.

5.  SF-IV40 skin flap surgery irradiated with 780 nm laser, 40 J/cm$^2$.

## 2.2. Collection of skin sample

Skin samples were collected on the seventh day after surgery. In order to standardize sample collection, skin tissue was obtained at the borderline between viable tissue characterized by soft skin (reddish, warm, and haired) and necrotic tissue (stiff, dark, cool, and hairless) (Fig. 1F). This tissue was divided into three parts: right, central and left. The right piece was used for western blotting and zymography assay. The central piece was fixed in formalin and used in histological analysis.

## 2.3. Blood vessels count

We performed morphometric analysis in order to estimate the number of blood vessels in the skin after the procedures. The skin tissue was fixed in formalin (10%) and embedded in paraffin. Sections of 6 μm were cut and stained with the hematoxylin and eosin method (HE). Blood vessel count was performed with light microscopy on a total of three nonconsecutive sections per rat. Photographs were taken under optical microscopy (Zeiss Germany; magnification ×400). We analyzed two slices per animal (18 fields per slide). An average of two slices per animal was used for statistical analysis. The number of animals was 12 per group.

All blood vessels present in tissue were counted without distinguishing their nature (arterioles, venules and capillaries). Histological analysis was performed by two independent investigators blinded to treatment. Data represent the mean of the fields analyzed by both investigators. Pictures were analyzed and blood vessels were quantified using Image J software (NIH, Bethesda, USA).

## 2.4. Immunoblotting – HIF-1α protein expression

Frozen tissue (100 mg) was pulverized in liquid nitrogen with a mortar and pestle. Samples were homogenized in radio immune precipitation assay buffer containing 10-mM Tris-HCl (pH 7.5), 1% Tergitol, 0.1% sodium dodecyl sulfate (SDS), 1% sodium deoxycholate, 150 mMNaCl, and proteolytic enzyme inhibitors (40 μg/mL phenylmethylsufonylfluoride and 10 μg/mL pepstatin; Sigma). After debris separation by centrifugation for 45 min at 14,000$g$, the supernatants were collected and protein concentration was determined by the Bradford

method (Bio-Rad Laboratories, Hercules, CA, USA). Samples were stored at −80 °C until assayed.

Proteins were analyzed by SDS-polyacrylamide gel electrophoresis under reducing conditions. Tissue extracts (50 μg) were boiled in equal volumes of loading buffer (150 mM Tris-HCl–pH 6.8, 4% SDS, 20% glycerol, 15% β-mercaptoethanol, and 0.01% bromophenol blue) and were subjected to electrophoresis in 9% non-denaturing polyacrylamide gels. Following electrophoretic separation, proteins were transferred to Hybond-P membranes (Amersham Pharmacia Biotech, Buckinghamshire, England). Membranes were blocked with 5% non-fat dry milk in Tris-buffered saline and 0.5% Tween 20 (TBST) for 1 h. Primary antibody (Ab) against HIF-1α (rabbit polyclonal, 1:1000, Santa Cruz) was diluted in TBST with BSA 0.5% and incubated in 4 ° C overnight. After washing twice with TBST, secondary Ab horseradish peroxidase conjugate (Sigma Aldrich) was applied at dilution 1:1000 for 1 h. Blots were washed in TBST twice over 30 min and were incubated in enhanced chemiluminesence reagents Super signal detection kit GBox Gel Document System. Band intensity was quantified using Gene Tools software (Syngene, USA).

## 2.5. Real time-PCR

Real time reverse transcription polymerase chain reaction (RT-PCR) was used to determine messenger RNA (mRNA) levels in the skin tissue. Total RNA was extracted from frozen rat skin with TRIzol reagent (Invitrogen, Carlsbad, CA) following the manufacturer's instructions. RNA was dissolved in diethyl pyrocarbonate treated water and quantified spectrophotometrically at 260 nm. Two nanograms mRNA were used for real-time PCR. The amplification was performed in a thermal cycler (Applied BiosystemsStepOne ™) at 50 °C for 10 min, 95 °C for 5 min and then 95 °C for 15 s followed by 60 °C for 30 s, and 72 °C for 30 s for 40 cycles. Real-time PCR was performed in a 15 μL reaction mixture containing 7.5 μL 2× SYBR Green Reaction Mix (Invitrogen), 0.3 μL each primer, 0.3 μL Super Script III RT/Platinum Taq Mix (10 pmol/μl), 0.15 μL ROX Reference Dye, and 5 μL sample in water. The sequences of the specific primers (Invitrogen) and reaction conditions used for RT-PCR are the following: for rat GAPDH (forward: GATGCTGGTGCTGAGT-ATGTCG; reverse: TGGTGCAGGATG-CATTGCTGA); VEGF (forward: TGCACCCACGACAGAAGG; reverse: GCACACAG-GACGGCTTGA) genes.

## 2.6. Gelatin zymography – MMP-2 activity

Twenty-microgrms of the supernatants from tissue extract were applied to 10% polyacrylamide gels with 1% gelatin incorporated as a substrate for gelatinolytic proteases. After running the gel, the SDS was removed by washing the gel twice in 2.5% (vol/vol) Triton X-100 (Sigma) for 30 min. The gel was incubated over-night in zymography development buffer containing 50 mM of Tris-HCl (pH 7.4), 2 mM of NaN$_3$, and 5 mM of CaCl$_2$. After development, the gels were stained for 3 h in 45% methanol/10% glacial acetic acid containing 1% (wt/vol) Coomassie Blue R-250 (Bio-Rad Laboratories) and were subsequently partially destained with the same solution without dye. To confirm identity of specific gel bands, recombinant control for latent and active MMP-2 was electrophoresed next to the tissue extracts. The gelatinolytic activity of each MMP was qualitatively evaluated as a clear band against the blue-stained gelatin background. Band intensity was quantified by using Gene Tools software (Syngene, USA). The activity of both the latent and active MMP-2 bands was measured separately and results represent the active-to-latent ratio (OD of active form/OD of latent form).

## 2.7. Statistical analysis

Data were expressed as mean ± SEM. Comparisons between experimental groups were performed by analysis of variance (ANOVA), and Student Newman Keuls test was used as

post-hoc test to compare individual groups (groups were compared 3 with 3). A $p < 0.05$ was considered significant. All analyses were performed using GraphPadInstat Software (V. 3.05, San Diego, CA, USA). We performed comparisons among different fluences for the same wavelength.

## 3. Results

### 3.1. Effect of laser irradiation on angiogenesis on skin flap

Initially we evaluated the effects of 660 nm or 780 nm wavelength laser irradiation on vessel formation in skin flaps. There was a marked increase in angiogenesis in samples from irradiated animals compared to samples from control rats, as observed in Fig. 2A, where photomicrographs obtained from histological sections stained with H&E are depicted. The numerical quantification of these data is shown in Fig. 2B and C, where we can observe that both laser wavelengths used enhanced new vessel formation. It is necessary to note that, in this study, we compared different fluencies of the same wavelength laser and we did not compare different wavelengths at the same fluence.

The 660 nm laser (Fig. 2B1) at the fluence of 40 $J/cm^2$ (SF-R40) provided an increase in the number of vessels in the skin flap when compared to groups SF-NI ($p < 0.001$) and SF-R30 ($p < 0.01$). The group irradiated with 660 nm laser at the fluence of 30 $J/cm^2$ did not showan increase in the number of vessels when compared to the non-irradiated group (SF-NI). Both fluences of 30 $J/cm^2$ and 40 $J/cm^2$ of 780 nm laser increased the number of vessels in the skin flap ($p < 0.001$ vs SF-NI) (Fig. 2B2).

These data confirm the results from other previous studies by our group showing that LLLT irradiation enhances new vessels formation. We further sought for the mechanism that could be responsible for this phenomenon.

### 3.2. Effect of laser irradiation on vascular endothelial growth factor mRNA expression

We evaluated VEGF mRNA expression in all experimental groups (Fig. 3). LLLT at 660 nm and 780 nm wavelengths enhanced VEGF mRNA expression levels at both fluences compared to non-irradiated control group (SF-NI). Irradiation with 660 nm laser increased VEGF gene expression (Fig. 3A) both at the fluence of 30 $J/cm^2$ ($p < 0.01$ vs SF-NI) and 40 $J/cm^2$ ($p < 0.001$ vs SF-NI) when compared to group SF-NI. A similar result was obtained with 780 nm laser (Fig. 3B): there was an increase in VEGF gene expression both at the fluence of 30 $J/cm^2$ ($p < 0.01$ vs SF-NI) and 40 $J/cm^2$ ($p < 0.001$ vs SF-NI).

### 3.3. Effect of laser irradiation on matrix metalloproteinase-2 (MMP-2) activity

MMP expression and activity are involved in the angiogenic process. Therefore, we evaluated the effects of different fluences of 660 nm and 780 nm laser on MMP-2 activity in our experimental model (Fig. 4).

The zymographic analysis showed differences in the proteolytic MMP-2 activity (Fig. 4A and B). There were no significant differences in active-to-latent MMP-2 ratio between different groups or fluences for both 600 nm and 780 nm. Although there was no statistical difference in MMP-2 activity, in groups irradiated with 660 nm (Fig. 4A) and 780 nm (Fig. 4B) lasers, the MMP-2 activity decreased in group SF-40 when compared to group SF-NI and also compared to the group irradiated with 30 $J/cm^2$. These results suggest that in groups irradiated with 40 $J/cm^2$ undergo less intense tissue degradation/remodeling mediated by MMP-2 activity.

Interestingly, there seems to be a direct relationship between MMP-2 activity and the fluences could be observed, since both 40 J/cm$^2$ groups showed lower MMP-2 activity than their respective 30 J/cm$^2$ counterparts. Taken as a whole, these results indicated that, in this model, MMP-2 activity was dependent on the fluences, regardless of the wavelengths used.

### 3.4. Effect of laser irradiation on hypoxia inducible factor-1α (HIF-1α) protein expression

Since we observed increased vessel formation in skin flaps, and it is well known that the angiogenic process is stimulated by hypoxia, we further tested the hypothesis that the beneficial effect of laser could be due to activation of the transcription factor HIF-1α. The results revealed that the non-irradiated SF-NI group expressed HIF-1α. In the 660 nm irradiated group, there was a clear enhanced expression of HIF-1α, detected even at the lower fluence tested (Fig. 5A; $p < 0.01$ vs SF-NI). This phenomenon was less evident in the 780 nm-treated animals, where the results were more erratic and no significance was obtained (Fig. 5B). Altogether, these results suggest that HIF-1α could be responsible, at least in part, for some of the beneficial effects of laser therapy on skin flaps.

## 4. Discussion

LLLT is a therapeutic approach with broad clinical applications, particularly in the treatment of inflammatory diseases or for enhancing wound healing. From previous studies from our laboratory, it has become clear that increased angiogenesis is one of the main processes by which LLLT may exert its beneficial effects. A precise mechanism for this phenomenon is still lacking. In this study, we report that, in an experimental model of skin flaps in rats, LLLT induced angiogenesis through several molecular mechanisms, by increasing HIF-1α and VEGF expression and by modulating MMP-2 activity.

We observed a marked increase in the number of vessels in the skin flap in animals that were irradiated. These results confirmed the findings reported by other authors. *In vivo* studies in different models such as myocardial infarct [10,15] and wound healing [11], have shown evidence that LLLT induced a similar effect on angiogenesis. Since these previous studies reported a crucial role for VEGF on this phenomenon [10,11,15,16], we further sought for VEGF expression in our experimental model of ischemic skin flaps. We observed that the non-irradiated flaps expressed low amounts of VEGF mRNA, probably as an adaptive response to the tissue hypoxia. In LLLT treated flaps, there was a marked increase in VEGF mRNA transcription, observed with both wavelengths used regardless of the fluences. We therefore concluded that VEGF photobiostimulation is a mechanism through which 660 nm and 780 nm lasers induce tissue revascularization.

We then expanded our study, looking for other mediators that could be affected by LLLT and thereby enhance angiogenesis.

It is known that the angiogenesis process is initiated by the activation of endothelial cells, followed by proteolysis of basement membrane, enabling abluminal sprout formation, cellular proliferation, and growth of the new vessels [17]. In this process, the crucial step of extracellular matrix (ECM) degradation is performed by matrix metalloproteinases (MMPs). MMPs are a family of 28 endopeptidases that selectively degrade ECM components. These enzymes are produced by a variety of cell types, including fibroblasts, epithelial, smooth muscle, endothelial, and inflammatory cells [17–19]. The activity of MMPs is necessary for vascular basement membrane degradation and ECM remodeling in order to allow the migration of endothelial cells [17,19] during angiogenesis.

Specifically, we quantified MMP-2 gelatinolytic activity through zymography and observed that the proteolytic activity was dose-dependent in both wavelengths used. In the groups

irradiated with 660 nm and 780 nm, there was an evident decrease in MMP-2 activity only at the fluence of 40 J/cm$^2$. Although, the MMP-2 activity was less intense at the fluence of 40 J/cm$^2$ than the 30 J/cm$^2$ groups there were no significant between theirs. Does the laser have a direct action on MMP-2 activity or is it an indirect effect based on the increase (or maturity) in blood vessels. We saw that the activity of MMP-2 was decreased while there was an increase in the number of vessels in the tissue.

Under normal conditions, the maintenance of the ECM is a dynamic process in which the deposition of ECM proteins is balanced by MMPs protein degradation. Differently, in states of excessive tissue remodeling when proteolysis surpasses protein deposition, wound healing could be impaired. MMPs are secreted as latent proenzymes that can be activated by different mechanisms including other MMPs as well as reactive oxygen species (ROS) and reactive nitrogen species (RNS) [20–22]. The regulation of MMP activity occurs at many levels, including, proenzyme activation, post-transcriptional modification (e.g. s-nitrosation [21]) and an additional control that occurs by the family of tissue inhibitors of metalloproteinases (TIMPs).

Endothelial cells constitutively secrete pro-MMP-2, and the exposure of these cells to type I collagen after disruption of the basement membrane or exposure to pro-inflammatory cytokines such as TNF-α can increase the expression of MT1-MMP (Membrane Type 1 – Matrix Metalloproteinase), which can then induce the activation of pro-MMP-2 [19]. Nevertheless it is evident that control of MMP-2 activity is involved either upstream or downstream of the angiogenic process induced by LLLT.

Although the exact mechanism is unknown, the final pathway of the photobiostimulation process seems to be the modification of the gene response. The measurement of this response can be seen through gene expression and production of proteins that mediate inflammatory and healing responses. Thus, we decided to analyze the LLLT effect on the main transcription factor activated during hypoxia, known as HIF-1α.

Cellular adaptation to the lack of oxygen is mediated by transcription factor HIF-1α. This protein is stabilized at low oxygen tensions while at higher oxygen tensions it is rapidly degraded by prolyl hydroxylase enzymes that are oxygen dependent. HIF-1α regulates the cellular response to physiological and pathological hypoxiaby activating genes that are important to cellular adaptation and survival pathways under hypoxic conditions [6,23]. Among the target genes of this transcription factor, VEGF, VEGFr, glucose carrier (GLUT1), and phosphoglycerate kinase (PGK) enzyme [24] are all important. In our experimental model, we observed that the non-irradiated group expresses HIF-1α in response to tissue hypoxia. In irradiated groups, only 660 nm laser is able to increase HIF-1α expression in this model regardless of the fluence used.

An interesting fact was that increased HIF-1α expression and the consequent induction of mRNA for VEGF occurred at the fluence of 30 J/cm$^2$ (660 nm), but we did not notice a significant increase in the number of vessels in this group. In this case, it is possible that 660 nm laser effect on angiogenesis depends on the dose applied to the tissue. The fluence of 30 J/cm$^2$ of 660 nm laser although it increased pro-angiogenic signals in the skin flap even after seven days, was. However insufficient to induce the formation of new vessels. The higher fluence (40 J/cm$^2$) of 660 nm however did induce new vessels while also inducing increases in MMP-2 activity as well as the increases in VEGF and HIF-1α. This might lead one to suppose that MMP-2 activity was critical for new vessel formation.

LLLT involves a wide range of complex interacting parameters such as wavelength, total fluence, fluence rate, coherence, pulse structure and pulsed or continuous wave [4,25]. Different studies have proven the biphasic dose-response concept related both to total

energy density and power density delivered to the tissue and it has been observed that there can is optimal light dose for a specific application. Doses both higher or lower than these optimal values can, in some cases, have reduced therapeutic efficiency [25–27].

When analyzing the 660 nm laser effect at the fluence of 40 J/cm$^2$, we confirm that HIF-1$\alpha$ is a signaling pathway involved in the increased angiogenesis in this model. LLLT increased the number of vessels in the tissue concomitantly with the increases in HIF-1$\alpha$ and VEGF expression. It can be concluded HIF-1$\alpha$ induction after LLLT does not occur due to a negative effect on the tissue, for instance, reducing even more the local oxygen tension, because we did not notice any difference in the necrosis area of these animals [4]. HIF-1$\alpha$ expression is primarily induced by hypoxia, but its induction can also be mediated by growth factors and cytokines. In this case, the induction does not depend on the oxygen tension and involves the activation of a different regulatory mechanism possibly mediated by mitogen-activated protein kinase and phosphatidylinositol 3-kinase/Akt signaling pathway [28]. Oxidative stress can also increase the expression of this transcription factor in the tissues.

When analyzing the results, we noticed that 780 nm laser did not increase HIF-1$\alpha$ expression as much as 660 nm laser did. Thus, it is possible that 780 nm laser regulates angiogenesis through the modulation of other transcription factors such as activator protein-1 (AP-1) and signal transducer and activator of transcription-3 (STAT3) [29]. It is also possible that HIF-1$\alpha$ protein could be stabilized within the cell [5,23].

As the treatment did not change the injured area in this model, [4], we did not compare the efficiency of either wavelength in relation to angiogenesis induction. However, we observed that both wavelengths could induce angiogenesis possibly through different cellular signaling mechanisms. In short, our data indicate that 660 nm laser at 40 J/cm$^2$ induced angiogenesis via HIF-1$\alpha$, followed by an increase in VEGF mRNA and formation of new vessels in the tissue. We also verified that these effects are dose-dependent because although 30 J/cm$^2$ gave increased HIF-1$\alpha$ and VEGF mRNA there was no increase in new vessel formation. With 780 nm laser, we verified its potential to increase tissue vascularization by inducing VEGF mRNA. However, we did not see any relation with increased HIF-1$\alpha$.

We showed that LLLT could improve the healing of skin flaps by enhancing the amount of new vessels formed in the tissue. Moreover, several mechanisms seem to be implicated in this phenomenon, namely, enhanced VEGF secretion and HIF-1$\alpha$ expression, accompanied by a decrease in MMP-2 activity. Considering these results, it seems unlikely that a single molecular process is responsible for all LLLT actions in angiogenesis and healing. Photostimulation may affect several independent cell-signaling pathways. More studies are necessary to confirm dose, wavelength, and total energy parameters needed for achieving the optimum biological effect and to confirm the molecular mechanisms activated by LLLT.

## Acknowledgments

## References

1. Kerrigan CL. Skin flap failure: pathophysiology. Plast. Reconstr. Surg. 1983; 72:766–777. [PubMed: 6647600]

2. Pinfildi CE, Liebano RE, Hochman BS, Ferreira LM. Helium–neon laser in viability of random skin flap in rats. Lasers Surg. Med. 2005; 37:74–77. [PubMed: 15954113]

3. Bossini PS, Fangel R, Habenschus RM, Renno AC, Benze B, Zuanon JA, Neto CB, Parizotto NA. Low-level laser therapy (670 nm) on viability of random skin flap in rats. Lasers Med. Sci. 2009; 24:209–213. [PubMed: 18351431]

4. Cury V, Bossini PS, Fangel R, Crusca Jde S, Renno AC, Parizotto NA. The effects of 660 nm and 780 nm laser irradiation on viability of random skin flap in rats. Photomed. Laser Surg. 2009; 27:721–724. [PubMed: 19803711]

5. Fang J, Yan L, Shing Y, Moses MA. HIF-1α-mediate up-regulation of vascular endothelial growth factor, independent of basic fibroblast growth factor, is important in the switch to the angiogenic phenotype during early tumorigenesis. Cancer Res. 2001; 61:5731–5735. [PubMed: 11479208]

6. Botusan IR, Sunkari VG, Savu O, Catrina AI, Grunler J, Lindberg S, Pereira T, Yla-Herttuala S, Poellinger L, Brismar K, Catrina SB. Stabilization of HIF-1α is critical to improve wound healing in diabetic mice. Proc. Natl. Acad. Sci. USA. 2008; 105:19426–19431. [PubMed: 19057015]

7. Conway EM, Collen D, Carmeliet P. Molecular mechanisms of blood vessel growth. Cardiovasc. Res. 2001; 49:507–521. [PubMed: 11166264]

8. Pinheiro AL, Meireles GC, de Barros Vieira AL, Almeida D, Carvalho CM, dos Santos JN. Phototherapy improves healing of cutaneous wounds in nourished and undernourished Wistar rats. Braz. Dent. J. 2004; 15:SI21–SI28. [PubMed: 15690767]

9. Ankri R, Lubart R, Taitelbaum H. Estimation of the optimal wavelengths for laser-induced wound healing. Lasers Surg. Med. 2010; 42:760–764. [PubMed: 20886508]

10. Tuby H, Maltz L, Oron U. Implantation of low-level laser irradiated mesenchymal stem cells into the infarcted rat heart is associated with reduction in infarct size and enhanced angiogenesis. Photomed. Laser Surg. 2009; 27:227–233. [PubMed: 19382832]

11. Corazza AV, Jorge J, Kurachi C, Bagnato VS. Photobiomodulation on the angiogenesis of skin wounds in rats using different light sources. Photomed. Laser Surg. 2007; 25:102–106. [PubMed: 17508845]

12. Correa F, Lopes Martins RA, Correa JC, Iversen VV, Joenson J, Bjordal JM. Low-level laser therapy (GaAs lambda = 904 nm) reduces inflammatory cell migration in mice with lipopolysaccharide-induced peritonitis. Photomed. Laser Surg. 2007; 25:245–249. [PubMed: 17803379]

13. Mesquita-Ferrari RA, Martins MD, Silva JA Jr, da Silva TD, Piovesan RF, Pavesi VC, Bussadori SK, Fernandes KP. Effects of low-level laser therapy on expression of TNF-α and TGF-β in skeletal muscle during the repair process. Lasers Med. Sci. 2010

14. Prado RP, Liebano RE, Hochman B, Pinfildi CE, Ferreira LM. Experimental model for low level laser therapy on ischemic random skin flap in rats. Acta Cir. Bras. 2006; 21:258–262. [PubMed: 16862348]

15. Tuby H, Maltz L, Oron U. Modulations of VEGF and iNOS in the rat heart by low level laser therapy are associated with cardioprotection and enhanced angiogenesis. Lasers Surg. Med. 2006; 38:682–688. [PubMed: 16800001]

16. Kipshidze N, Nikolaychik V, Keelan MH, Shankar LR, Khanna A, Kornowski R, Leon M, Moses J. Low-power helium: neon laser irradiation enhances production of vascular endothelial growth factor and promotes growth of endothelial cells in vitro. Lasers Surg. Med. 2001; 28:355–364. [PubMed: 11344517]

17. Rivilis I, Milkiewicz M, Boyd P, Goldstein J, Brown MD, Egginton S, Hansen FM, Hudlicka O, Haas TL. Differential involvement of MMP-2 and VEGF during muscle stretch – versus shear stress-induced angiogenesis. Am. J. Physiol. Heart Circ. Physiol. 2002; 283:H1430–H1438. [PubMed: 12234794]

18. Stetler-Stevenson WG. Matrix metalloproteinases in angiogenesis: a moving target for therapeutic intervention. J. Clin. Invest. 1999; 103:1237–1241. [PubMed: 10225966]

19. Nguyen M, Arkell J, Jackson CJ. Human endothelial gelatinases and angiogenesis. Int. J. Biochem. Cell Biol. 2001; 33:960–970. [PubMed: 11470230]

20. Lizarbe TR, Garcia-Rama C, Tarin C, Saura M, Calvo E, Lopez JA, Lopez-Otin C, Folgueras AR, Lamas S, Zaragoza C. Nitric oxide elicits functional MMP-13 protein-tyrosine nitration during wound repair. FASEB J. 2008; 22:3207–3215. [PubMed: 18495757]

21. Gu Z, Kaul M, Yan B, Kridel SJ, Cui J, Strongin A, Smith JW, Liddington RC, Lipton SA. S-nitrosylation of matrix metalloproteinases: signaling pathway to neuronal cell death. Science. 2002; 297:1186–1190. [PubMed: 12183632]

22. Paduch R, Walter-Croneck A, Zdzisinska B, Szuster-Ciesielska A, Kandefer-Szerszen M. Role of reactive oxygen species (ROS), metalloproteinase-2 (MMP-2) and interleukin-6 (IL-6) in direct interactions between tumour cell spheroids and endothelial cell monolayer. Cell Biol. Int. 2005; 29:497–505. [PubMed: 15893483]

23. Srinivas V, Zhu X, Salceda S, Nakamura R, Caro J. Hypoxia-inducible factor 1α (HIF-1α) is a non-heme iron protein implications for oxygen sensing. J. Biol. Chem. 1998; 273:18019–18022. [PubMed: 9660756]

24. Tang N, Wang L, Esko J, Giordano FJ, Huang Y, Gerber HP, Ferrara N, Johnson RS. Loss of HIF-1α in endothelial cells disrupts a hypoxia-driven VEGF autocrine loop necessary for tumorigenesis. Cancer Cell. 2004; 6:485–495. [PubMed: 15542432]

25. Demidova-Rice TN, Salomatina EV, Yaroslavsky AN, Herman IM, Hamblin MR. Low-level light stimulates excisional wound healing in mice. Lasers Surg. Med. 2007; 39:706–715. [PubMed: 17960752]

26. Skinner SM, Gage JP, Wilce PA, Shaw RM. A preliminary study of the effects of laser radiation on collagen metabolism in cell culture. Aust. Dent. J. 1996; 41:188–192. [PubMed: 8768644]

27. Enwemeka CS, Rodriguez O, Mendosa S. The biomechanical effects of low-intensity ultrasound on healing tendons. Ultrasound Med. Biol. 1990; 16:801–807. [PubMed: 2095010]

28. Carroll VA, Ashcroft M. Role of hypoxia-inducible factor (HIF)-1α versus HIF-2α in the regulation of HIF target genes in response to hypoxia, insulin-like growth factor-I, or loss of von Hippel–Lindau function: implications for targeting the HIF pathway. Cancer Res. 2006; 66:6264–6270. [PubMed: 16778202]

29. Hamik A, Wang B, Jain MK. Transcriptional regulators of angiogenesis. Arterioscler. Thromb. Vasc. Biol. 2006; 26:1936–1947. [PubMed: 16778118]
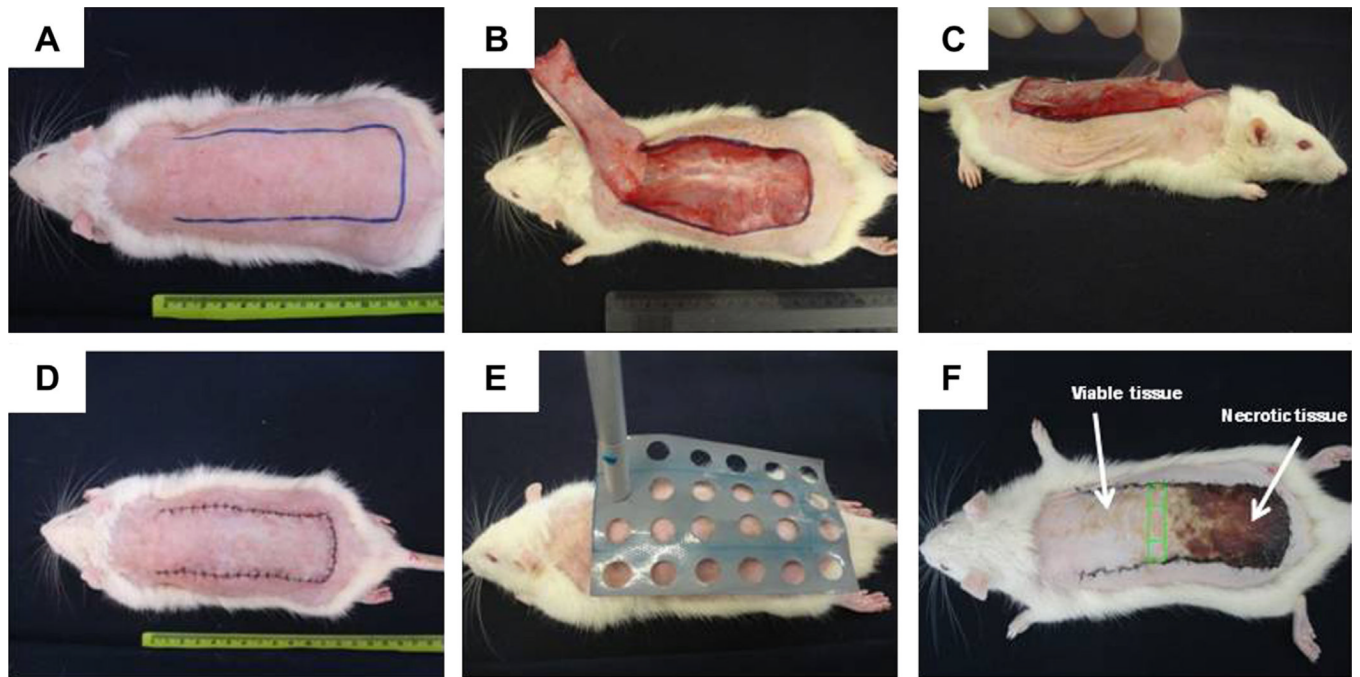
**Fig. 1.**
Dorsal skin flap surgical procedure and laser irradiation. (A) Outline of flap intended (10 × 4 cm). (B and C) Dorsal skin flap with cranial base with interposition of a plastic barrier. (D) Sutured flap after surgical procedure. (E) Template for laser irradiation with 24 points. (F) Green box at border of viable/necrotic tissue area was utilized for analyses. (For interpretation of the references to color in this figure legend, the reader is referred to the web version of this article.)
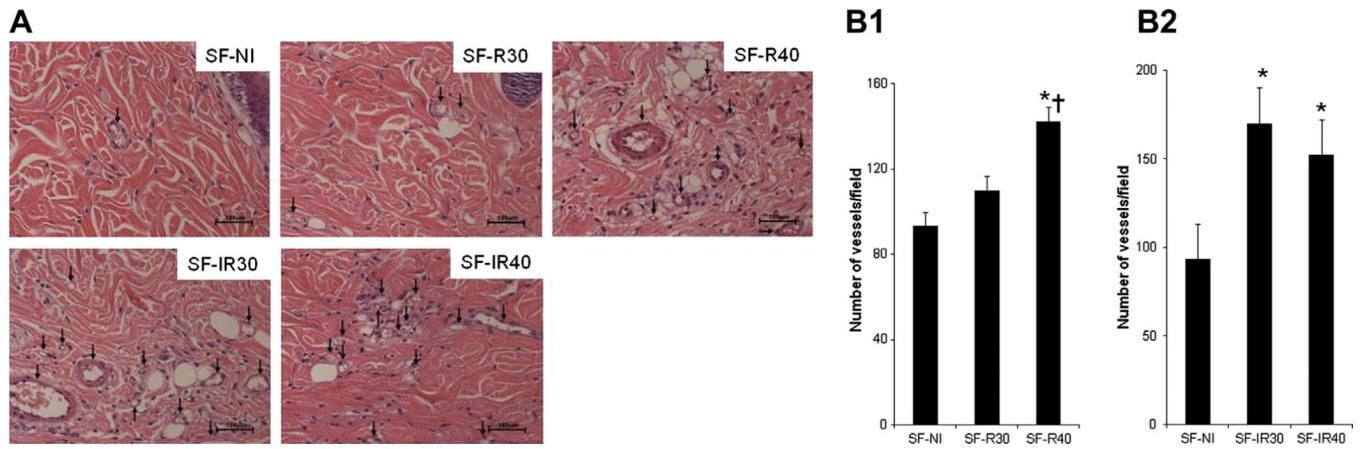
**Fig. 2.**
Effect of laser irradiation on angiogenesis. (A) Vessels (arrows) were identified by H&E tissue staining and (B) quantitatively expressed as a number of vessels per field on 7 days after skin flap surgery. (B1) Red laser group, $^*p < 0.001$ vs SF-NI and $^\dagger p < 0.01$ vs SF-R30; (B2) Infrared laser group, $^*p < 0.001$ vs SF-NI. Data expresses mean ± SEM. $n = 12$ animals per group.
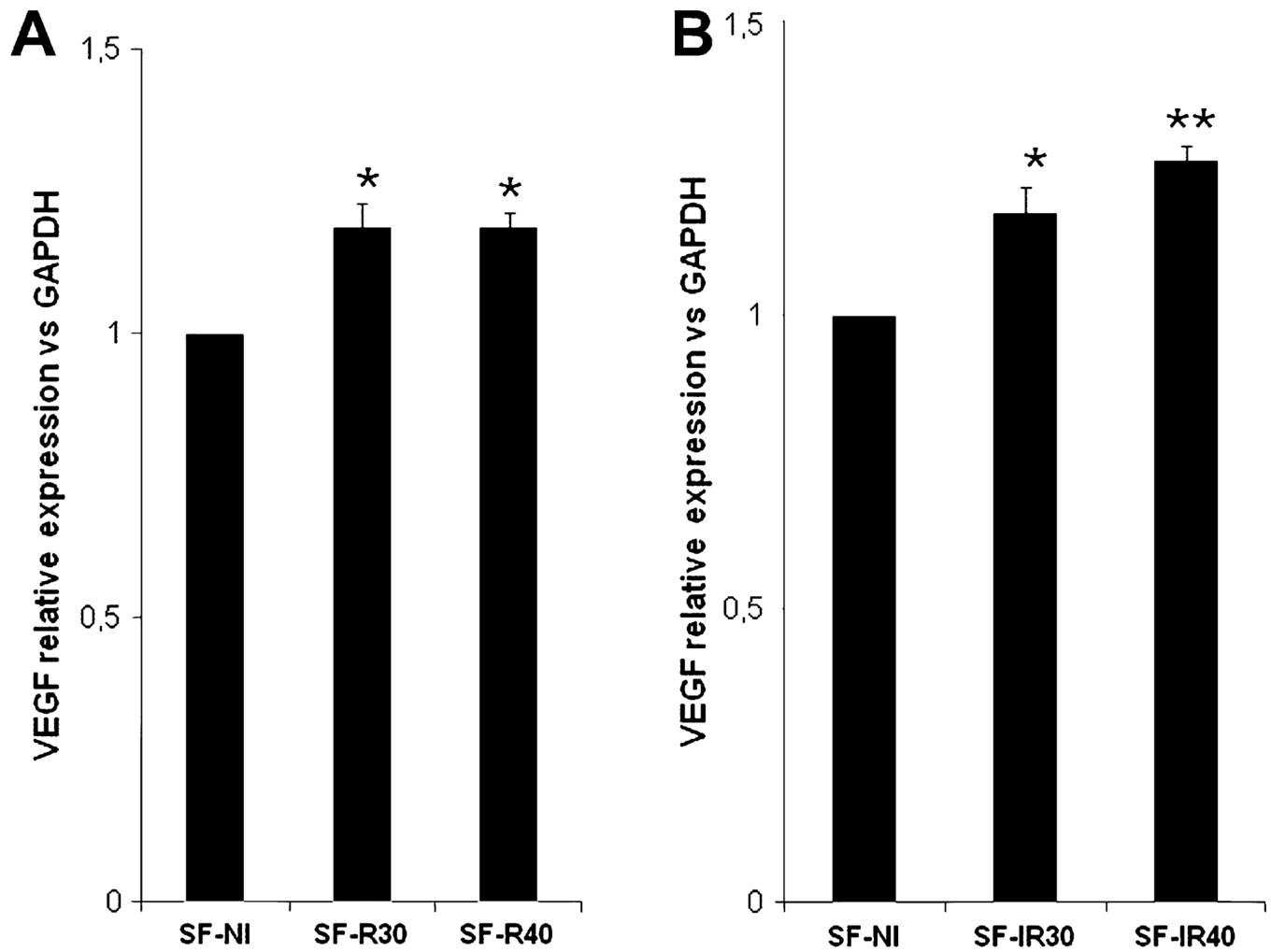
**Fig. 3.**
Effect of laser irradiation on VEGF mRNA expression. (A) VEGF mRNA expression normalized to GAPDH was increased in skin flap after red (A) and infrared (B) laser radiation.$^{*}p < 0.01$ and $^{**}p < 0.001$ vs SF-NI. Data expresses mean ± SEM. $n = 5$ animals per group.
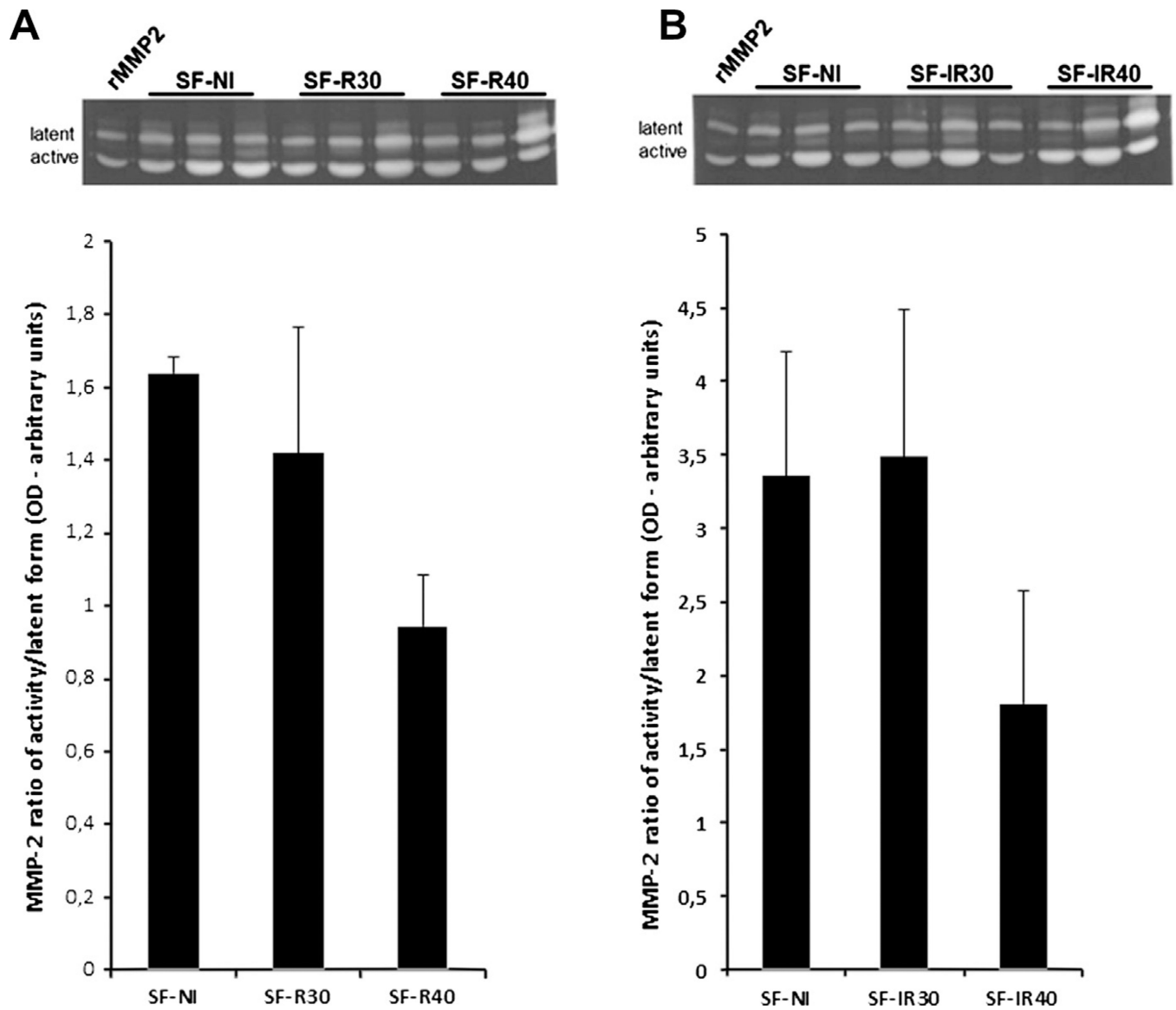
**Fig. 4.**
Effect of laser irradiation on MMP-2 activity. (A) MMP-2 activity in skin flap after red laser irradiation and (B) MMP-2 activity in skin flap after infrared laser radiation. Data expresses the active-to-latent ratio (mean ± SEM). $n = 3$ animals per group.
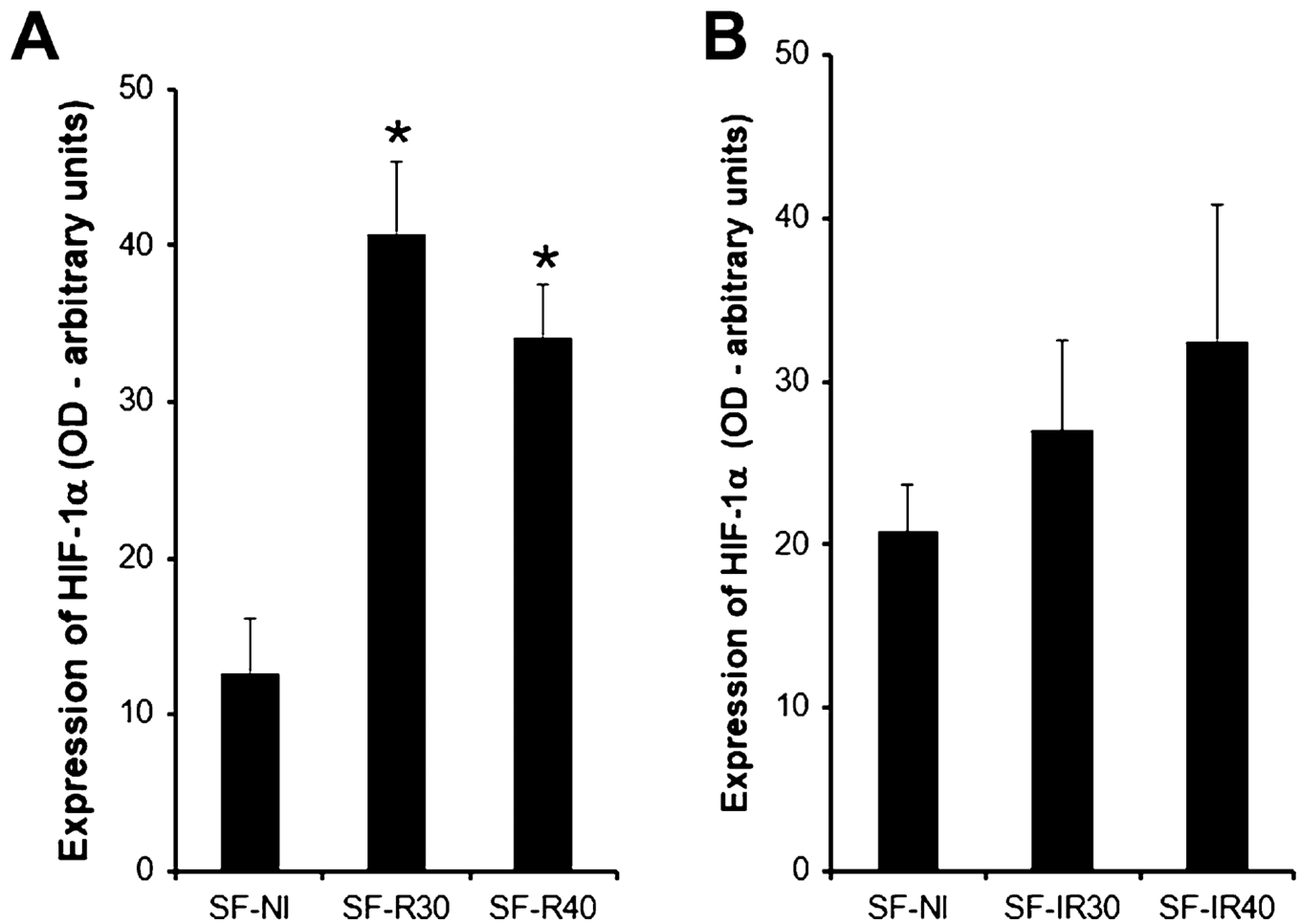
**Fig. 5.**
Effect of laser irradiation on HIF-1α protein expression. (A) Expression of HIF-1α was increased in skin flap after red laser radiation. $^{*}p < 0.01$ vs SF-NI. (B) Expression of HIF-1α in skin flap after infrared laser radiation. There were no differences between the groups. Data expresses mean ± SEM. $n = 3$ animals per group.